

## Effects of Dimethyl Sulfoxide and Mutations on the Folding of Aβ(25-35) Peptide: Molecular Dynamics Simulations

M. Ghobeh<sup>a</sup>, S. Ahmadian<sup>b,\*</sup>, M.B. Ebrahim-Habibi<sup>c</sup>, A.A. Meratan<sup>d</sup> and A. Ebrahim-Habibi<sup>e,f</sup>

<sup>a</sup>Department of Biology, Science and Research Branch, Islamic Azad University, Tehran, Iran

<sup>b</sup>Institute of Biochemistry and Biophysics, University of Tehran, P.O. Box: 14176114411, Tehran, Iran

<sup>c</sup>Microbiology and Biotechnology Research Group, Research Institute of Petroleum Industry, Tehran, Iran

<sup>d</sup>Department of Biological Sciences, Institute for Advanced Studies in Basic Sciences (IASBS), Zanjan, Iran

<sup>e</sup>Biosensor Research Center, Endocrinology and Metabolism Molecular-Cellular Sciences Institute, Tehran University of Medical Sciences, Tehran, Iran

<sup>f</sup>Endocrinology and Metabolism Research Center, Endocrinology and Metabolism Clinical Sciences Institute, Tehran University of Medical Sciences, Tehran, Iran

(Received 18 March 2017, Accepted 15 July 2017)

### ABSTRACT

The 25-35 fragment of the amyloid β(Aβ) peptide is a naturally occurring proteolytic by-product of its larger parent molecule that retains the amyloid characteristics and toxicity of the full length parent molecule. Aggregation of this peptide occurs rapidly in aqueous solutions and thus characterization of its folding process is very difficult. In the present study, early stages of Aβ(25-35) folding were observed in the presence of two mutations (N27A and M35A) in pure water, before and after exposure to pure dimethyl sulfoxide (DMSO) by conducting molecular dynamics simulations. Hydrophobic mutations decreased flexibility in the peptides structures, and peptide terminal mutation resulted in more compactness and beta secondary structure formation. Meanwhile, pure DMSO dramatically reduced the peptides dynamics, and pre-treatment with pure DMSO caused reduction and delay in beta structure formation in all studied peptides. It is concluded that the introduction of dimethyl sulfoxide and hydrophobic terminal M35A mutation could notably affect the folding of Aβ(25-35).

**Keywords:** Amyloid beta(25-35) folding, Hydrophobicity, Dimethyl sulfoxide (DMSO), Molecular dynamics (MD) simulations

### INTRODUCTION

The importance of protein misfolding has become increasingly clear in the recent decades with the discovery of a link between this phenomenon and a number of human diseases, including Alzheimer's, Parkinson's, and Huntington's diseases [1,2]. Regarding this issue, variations in pH, temperature, organic solvent, and mutations are critical circumstances that disrupt the native structure of proteins [2,3]. Among the proteins identified as emerging threats of modern society, Amyloid-β(Aβ) peptide has received high attention for direct implication in the development of neurodegeneration in Alzheimer's disease

(AD) [4,5]. The aggregation of Aβ, which is 39-43 residues long, has been predicted to be structurally induced by both the turn in the 26-29 fragment [6] and the hydrophobic interactions in the 29-42 section [7]. Among all Aβ fragments studied so far, Aβ(25-35), with the sequence 25G-S-N-K-G-A-I-I-G-L-M35, possesses the essential residues for quick formation of insoluble aggregates [7]. Despite its short length, it forms large, mature β-sheet fibrils [8,9] and retains similar toxicity to that of the full-length parent molecule [10,11]. Accordingly, this peptide, which is naturally produced *in vivo* by brain proteases [10], has been proposed as the biologically active region of intact Aβ [12]. Furthermore, the presence and increased titer of serum antibodies against aggregates of Aβ(25-35) in patients with progressive AD has been reported [13], suggesting that

\*Corresponding authors. E-mail: sh.ahmadian@ut.ac.ir

A $\beta$ (25-35) may be related to AD pathogenicity [14]. By retaining both the physical and biological properties of its parent molecule, A $\beta$ (25-35) could therefore be a reliable representative of full-length A $\beta$  in structural and functional studies. However, high hydrophobicity and aggregation-prone characteristics of A $\beta$ (25-35) have considerably hampered characterization of its aggregation process [15-18]. To resolve these technical problems, a variety of protocols using different types of solvents have been proposed in order to control the pace of the initial conformation/folding process and the subsequent aggregation behavior of A $\beta$ (25-35) peptide [19,20]. Many published methods suggest preparation of stock solutions of A $\beta$  in dimethyl sulfoxide (DMSO), before dilution into an aqueous buffer medium, to induce proper folding [21,22]. Liquid DMSO is widely used as a polar solvent that mixes well with a wide molarity range of water. At high DMSO concentrations (above 75%), proteins are shown to completely unfold, due to disruptions of the intramolecular backbone hydrogen bonds [23,24], while no detectable effect is observed upon the secondary structure of proteins at lower DMSO concentrations [24]. Another advantage of DMSO over other organic solvents arises from its aprotic physical properties due to its small relative dielectric constant ( $\epsilon$ ) of 46.8 and high dipole moment (4.0 D). These characteristics enable DMSO to solubilize hydrophobic helical peptides [24].

In addition to the solvent effect on the peptide initial assembly, the amino acid sequence is also an important determinant of folding. Substitutions within the regions of the sequence crucial for proper folding can affect aggregation tendency of the whole sequence by altering hydrophobicity at the site of mutation [25-27]. Regarding A $\beta$ (25-35), mutation of Asn27 to Ala has produced a more hydrophobic analog with less aggregation propensity and toxicity. On the other hand, a replacement of Met35 with Ala has yielded a less hydrophobic, but more toxic peptide [25].

The aggregation-prone characteristic of A $\beta$ (25-35) has made it difficult to determine its initial conformational changes at atomic resolution by convenient methods such as solution NMR or X-ray crystallography, in different solvents. Therefore, computational studies of molecular dynamics (MD) simulations have been employed to gain an

insight into the secondary structure and folding properties of A $\beta$ (25-35) in various solvents and conditions [18,26,28]. In the present study, MD simulation runs were performed on A $\beta$ (25-35) peptide and two of its mutant forms (N27A and M35A) in order to examine the conformation of these peptides in pure water at physiological temperature (37 °C equal to 310 K) before and after being simulated in pure DMSO at room temperature (25 °C equal to 300 K). Selection of DMSO was based on laboratory protocols which require dissolving A $\beta$  peptides in 100% DMSO, at room temperature, before dilution into medium buffer [21]. Therefore, the laboratory protocols of first dissolving A $\beta$  peptides in 100% DMSO at room temperature (300 K) followed by the aggregation of A $\beta$ (25-35) peptides at physiological temperature (310 K) was simulated in this study. However, in this case, DMSO was completely removed from the system before simulating the peptides in pure water. No previous simulation studies have examined the folding of A $\beta$ (25-35) and its two mutants (M35A and N27A) in pure DMSO and no investigation has been accomplished yet on the effect of pre-treatment with DMSO prior to dissolving the peptides in water. This study, for the first time, could further help to unmask the structural changes occurring in experimental studies when pre-treating various forms of A $\beta$ (25-35) in pure DMSO. Therefore, our results are valuable for understanding the early-stage conformation of amyloidogenic A $\beta$ (25-35) peptide, at atomic level, in a physiological environment by pretreatment with DMSO and/or introducing mutations in order to determine the efficiency of the solvent and substitutions for inducing structural changes.

## MATERIALS and METHODS

### Simulation Details

The starting conformation for the simulation of the A $\beta$ (25-35) was taken from the NMR analysis (PDB entry 1QWP) [28]. The mutant forms (N27A and M35A) were made using Molecular Operating Environment (MOE 2012.10) software (Chemical Computing Group Inc., 1010 Sherbooke St. West, Suite #910, Montreal, QC, Canada, H3A 2R7, 2012). Three sets of simulations of 200 ns were performed on A $\beta$ (25-35) peptide and the mutants: in pure water at 310 K (equivalent to physiological temperature of

37 °C); in pure DMSO at 300 K (equivalent to room temperature of 25 °C); in pure water at 310 K after being simulated in pure DMSO by eliminating DMSO molecules. Each peptide was first centered in a cubic box while being 1nm away from each side of the box. Each box was then solvated with either the simple point charge (SPC) water [29] or DMSO [30] molecules. To neutralize the total charge of the peptide (positively-charged lysine and peptide N-terminal along with negatively-charged C-terminal), three solvent molecules were replaced with two Cl<sup>-</sup> and one Na<sup>+</sup> ions. All MD simulations and analyses of the resultant trajectories were performed using the GROMACS 4.5.4 simulation package [31] with the GROMOS96 53a6 force field [32]. After applying steepest descent energy minimization, each trajectory was run through an NVT ensemble and equilibrated for 100 ps. The temperature was kept constant at 300 and 310 K for DMSO- and water-containing systems, respectively, using V-rescale thermostat [33]. It was then followed by an NPT equilibration for 100 ps using the Parinello-Rahman barostat [34] to keep the pressure close to 1 bar. The LINCS algorithm [35] was used to constrain all bond lengths. Each simulation was run using a time-step of 2 fs. A grid system was applied for neighbor searching with the neighbor list generation after every 5 steps. A cut-off radius of 1.0 nm was used for both the neighbor list and van der Waal's interaction. Particle Mesh Ewald (PME) [36] was employed to calculate the electrostatic interactions with a grid spacing value of 0.16 nm and an interpolation order of 4. Periodic boundary conditions were also applied. Simulations were first equilibrated by 100 ps of MD followed by productive runs of 200 ns.

### Simulations Analyses

The secondary structure of the peptides was analyzed using the DSSP program [37]. Cluster analysis was performed using the linkage method and a cutoff root mean-square deviation (RMSD) of 0.1 nm. Clustering calculations were made at 250-ps intervals. The graphical images were produced by means of VMD 1.8.6 program [38].

## RESULTS

Molecular dynamics simulation approaches have

provided a possible way for an in-depth analysis of the effects of mutations and solvents on A $\beta$ (25-35) peptide structure [18,26,28]. In the study presented here, an MD simulation technique was employed to characterize the early events related to the structural changes of A $\beta$ (25-35) and its two mutant forms (N27A and M35A) in two different conditions: in pure water at 310 K, before and after being simulated in explicit DMSO at 300 K.

### Stability, Flexibility and Conformational Diversity Analyses

The overall stability changes were evaluated through calculating backbone Root Mean Square Deviation (RMSD) values over a period of 200-ns simulation time for all simulation systems (Fig. 1). In this respect, all depicted RMSD values of each peptide were calculated by comparison to the starting conformation. An extensive structural deviation was observed in the wild-type and mutant forms in water systems, with and without pre-simulation in DMSO. All peptides showed deviation values of ~0.2 to ~0.8 nm in water before simulation in DMSO, except for M35A which maintained RMSD values of ~0.6 to ~0.8 nm starting from the 100-ns simulation point for about 80 ns. The average RMSD values of  $0.55 \pm 0.15$ ,  $0.38 \pm 0.14$ , and  $0.59 \pm 0.19$  nm were respectively obtained for the wild-type, N27A, and M35A structures in water, before simulation in DMSO. On the other hand, pre-treatment with DMSO caused the wild-type, N27A, and M35A to retain lower average RMSD values of  $0.50 \pm 0.11$ ,  $0.35 \pm 0.12$ , and  $0.38 \pm 0.15$  nm, respectively, in water.

Overall, N27A retained the lowest value of average RMSD in all water systems. In DMSO, all samples presented lower RMSD values compared to those simulated in water (Fig. 1). M35A, relative to other peptides, maintained lower RMSD values in DMSO, reflecting higher stability of this mutant in this solvent. In other words, DMSO in combination with M35A mutation conferred a more pronounced stability enhancement as compared to M35A substitution alone in water.

To assess flexibility of the peptides in DMSO and water, their backbone Root Mean Square Fluctuations (RMSF) over the simulation time were calculated. As shown in Fig. 2, both termini of all peptides appeared more flexible in all water simulations compared to the runs in DMSO.

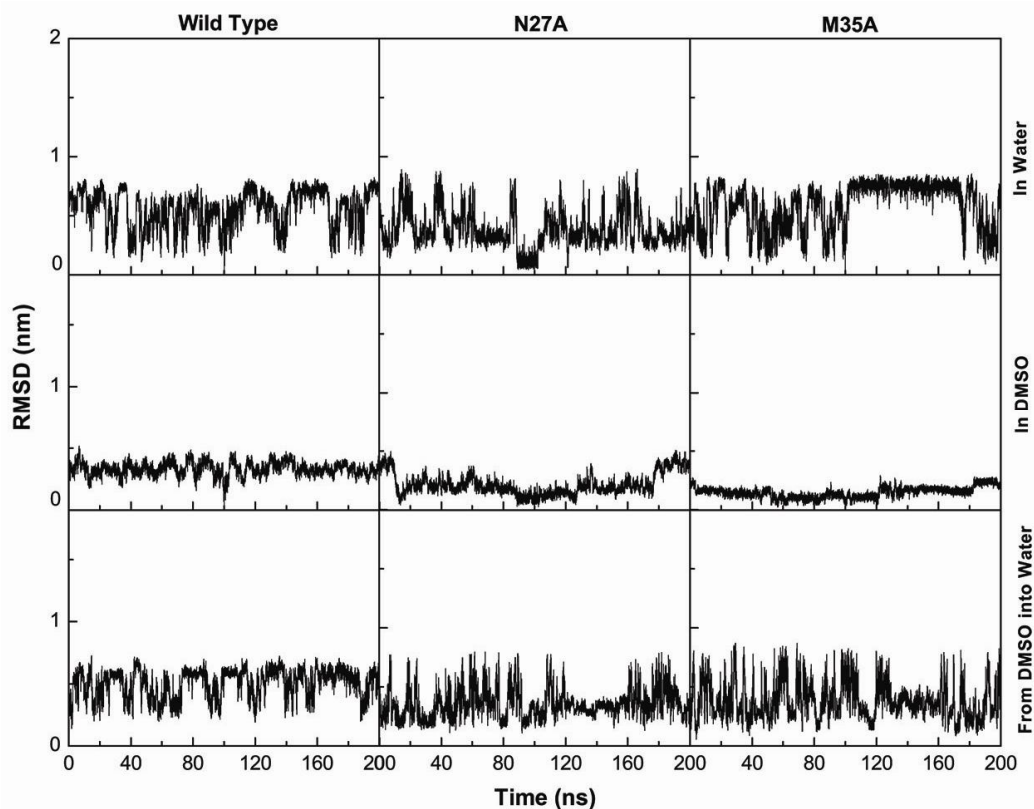


**Fig. 1.** Backbone RMSD of the wild-type and mutant structures of A $\beta$ (25-35). Changes in the RMSD for the backbone atoms of the wild-type (left column), N27A (middle column), and M35A (right column) peptide during the 200-ns MD simulations are shown in pure water (top row), pure DMSO (middle row), and from pure DMSO into pure water (bottom row). All depicted RMSD values of each peptide were calculated by comparison to the starting conformation.

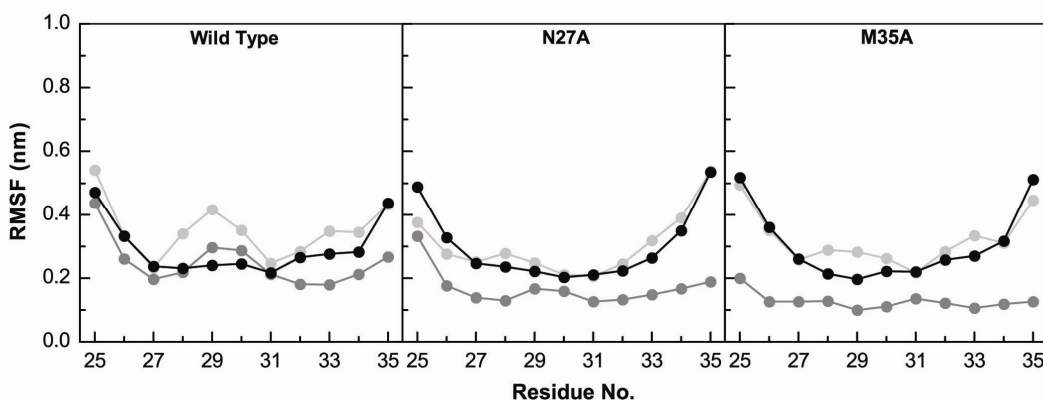


**Fig. 2.** Backbone RMSF calculated per residue of the wild-type and mutant structures of A $\beta$ (25-35) over the 200-ns simulation in pure water (light gray), pure DMSO (gray), and in pure water after being simulated in pure DMSO (black).

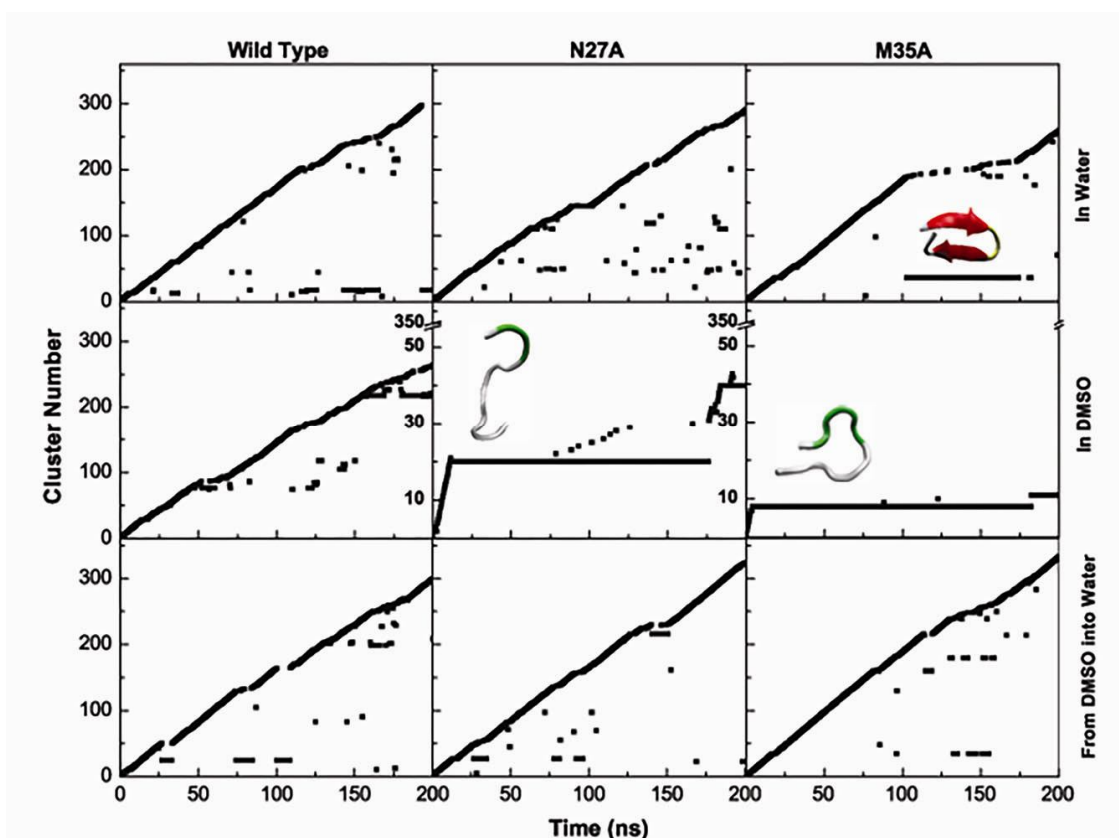


**Fig. 3.** Cluster analysis of the wild-type and mutant structures of Aβ(25-35). The time adopted by individual cluster of wild-type (left column), N27A (middle column), and M35A (right column) peptides during the 200-ns MD simulation are shown in pure water (top row), pure DMSO (middle row), and from pure DMSO into pure water (bottom row). The dominant conformations are depicted above the largest clusters. The N-terminal of the structures is positioned on top. White: coil; green: bend; yellow: turn; red: β-sheet.

Meanwhile, among pre-DMSO-treated peptides in water, both mutants demonstrated slightly higher flexibilities at their termini compared to the wild-type. However, the flexibilities of residues 29, 30, and 32 for both mutants were lower than those in the wild-type. Interestingly, after being DMSO-treated, residue 35 of M35A demonstrated a significant increase in its backbone RMSF compared to M35A in other two systems. Also, N27A mutant seemed to be less flexible in its central sequence compared to other peptides in pre-DMSO-treated water simulation leading to its greater stability. The backbone flexibility of all samples seemed to be the lowest in DMSO, as compared to both of water systems, except for Gly29 and Ala30 of the wild-type peptide which tended to be slightly higher in DMSO. In

general, both mutants demonstrated lower flexibilities in their central sequences in all simulation systems. As indicated in Fig. 2, among all simulation runs, residual flexibilities were significantly decreased related to M35A mutation when simulated in DMSO.

To investigate the conformational diversity of the peptides, a clustering analysis of the simulated trajectories was performed. Clustering method basically focuses on grouping structures which share similar conformational features. As shown in Fig. 3, the wild-type, N27A, and M35A structures exhibited 297, 291, and 259 distinct clusters, respectively, along the 200-ns-long simulation in pure water before simulation in DMSO. Among these samples, M35A demonstrated the least conformational

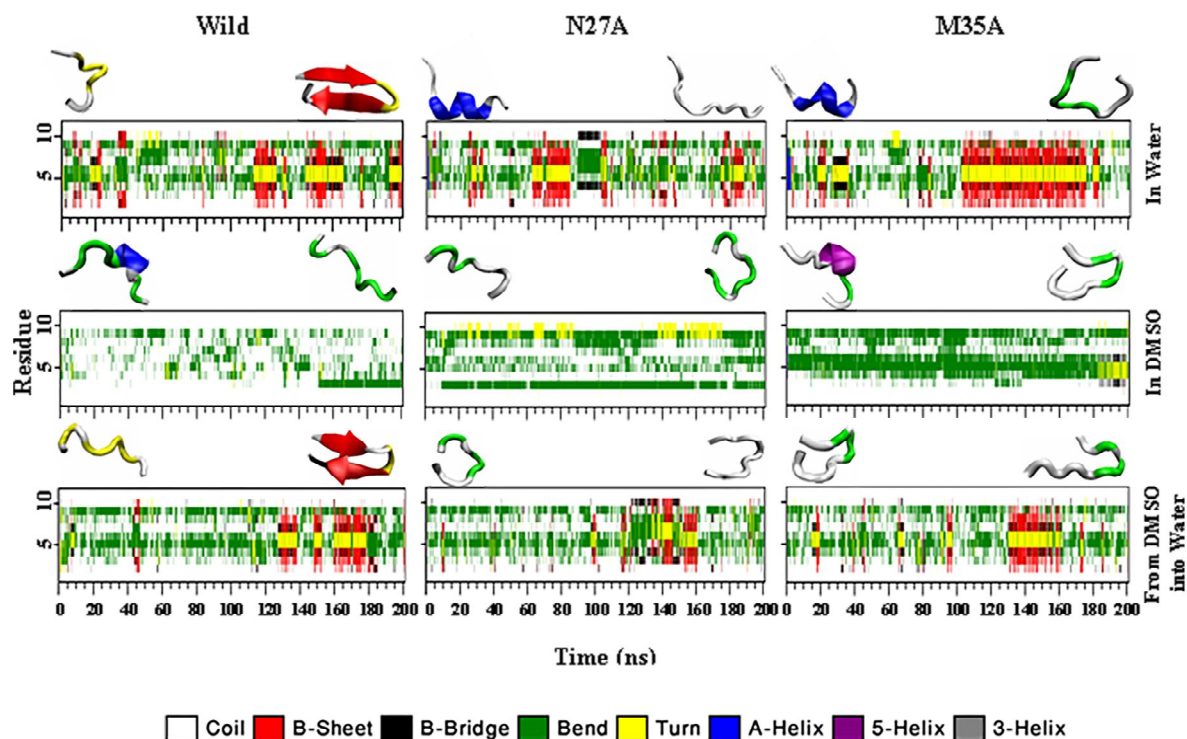


**Fig. 4.** Time course of the secondary structure for the simulations of the wild-type (left column), N27A (middle column), and M35A (right column) structures of  $A\beta(25-35)$  in pure water (top row), pure DMSO (middle row), and from pure DMSO into pure water (bottom row). Snapshots of the starting (from the 100-ps pre-simulation) and ending (after 200 ns simulation) structures are depicted. The N-terminal of the structures is positioned on top.

diversity with the largest cluster representing 38% of the trajectory and holding a  $\beta$ -strand structure. On the other hand, DMSO reduced conformational diversity in the wild-type, N27A, and M35A structures to 264, 43, and 11 clusters, respectively. In DMSO, N27A and M35A demonstrated lower conformational diversities, compared to the wild-type peptide, with their largest clusters maintaining dominantly random coil structure for 80% and 87% of their trajectories, respectively. When transferred from DMSO into water, the wild-type, N27A, and M35A structures exhibited higher conformational diversities by demonstrating 299, 324, and 333 distinct clusters, respectively, relative to those without being simulated in DMSO. Overall, M35A in DMSO retained the lowest number of clusters and thus highest stability among all simulations.

### Structural Analyses

Secondary structure analysis was performed using DSSP algorithm [37], which is based on the backbone geometry and the presence of hydrogen bonds. As shown in Fig. 4, in the initial water systems, the wild-type peptide and the mutants represented coil/turn and  $\alpha$ -helix in their starting structures, respectively, and  $\beta$ -sheets appeared in their structures throughout the simulation course. Therefore, introduction of the mutations in the wild-type sequence in the initial water system caused the formation of  $\alpha$ -helix instead of coil and turn in the starting structures of the mutants. On the other hand, in the final water simulations, pre-treatment with DMSO eliminated the mutants' initial  $\alpha$ -helix structures. Interestingly, the formation of  $\beta$ -sheet secondary structure was only observed in water simulations. In pure DMSO, the wild-type, N27A, and M35A peptides contained  $\alpha$ -helix, bend, and  $\pi$ -helix in their starting

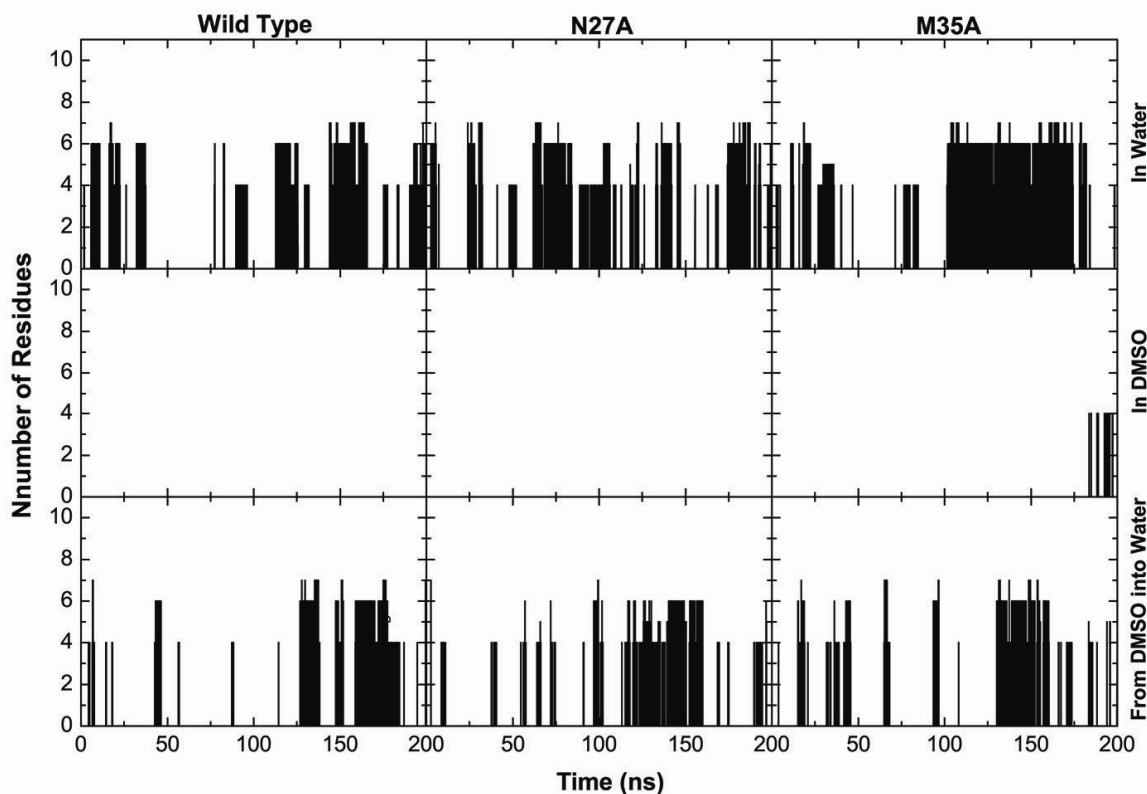


**Fig. 5.** Beta-sheet contents of the wild-type and mutant structures of A $\beta$ (25-35). Number of residues with beta-sheet structure are shown as bars during the 200-ns MD simulations for the wild-type (left column), N27A (middle column), and M35A (right column) peptides in pure water (top row), pure DMSO (middle row), and from pure DMSO into pure water (bottom row).

structures, respectively. DMSO seemed to abolish the formation of  $\beta$ -sheets in all peptides while coil and bend structures were dominant throughout the simulation time courses. In this case, the number of residues maintaining coil structure was higher for the wild-type peptide, whereas both mutants, especially M35A, acquired mostly bend structure. Meanwhile, DMSO caused a frequent presence of bend structure in residue N27A compared to the wild-type peptide. Overall, in DMSO, the wild-type peptide showed unfolding whereas N27A and M35A were adopting more compactness in their structures compared to mutants in initial water systems. The changes in  $\beta$ -sheet contents were also calculated separately for each simulation system (Fig. 5). After treatment with DMSO, the formation of  $\beta$ -sheets was significantly decreased in all three peptides. In final water simulations, pre-treatment with DMSO seemed to

cause general delay and significant reduction in  $\beta$  structure formation in all peptides compared to the non-treated ones (Figs. 4 and 5). Finally, in all simulations, both termini of all peptides formed mostly coil structure and were less stable, in accordance with RMSF analyses, indicating high flexibilities.

In order to further verify the structural changes in the peptides, the exact numbers of hydrogen bonds were calculated for each peptide throughout the simulation time course (Fig. 6). In initial water systems, the wild-type, N27A, and M35A structures exhibited an average H-bond numbers of 2.0, 1.6, and 2.3, respectively. In the initial water system, by holding a higher average H-bond number, M35A had a more compact structure compared to N27A, which is in accordance with DSSP results. In DMSO, average H-bond numbers decreased in the wild-type peptide

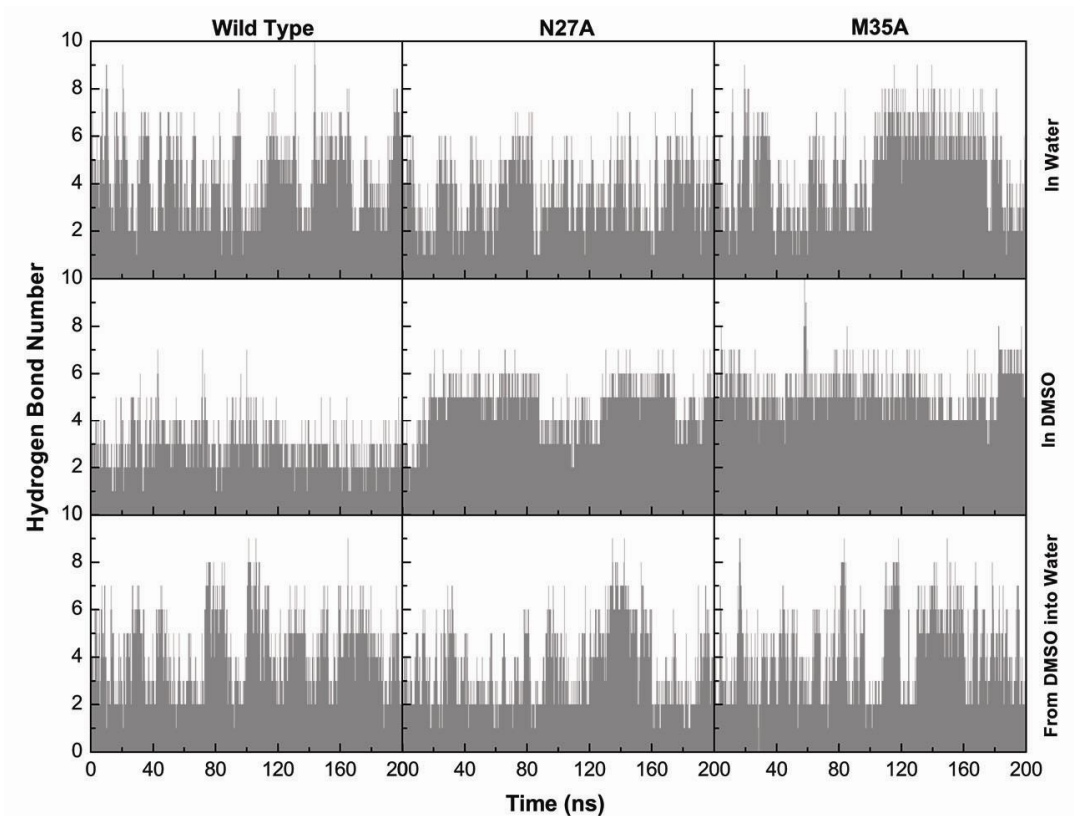


**Fig. 6.** Backbone hydrogen bonds of the wild-type and mutant structures of A $\beta$ (25-35). Number of hydrogen bonds during the 200-ns MD simulations are shown as bars for the wild-type (left column), N27A (middle column), and M35A (right column) peptides in pure water (top row), pure DMSO (middle row), and from pure DMSO into pure water (bottom row).

to 0.9 and increased in N27A and M35A to 2.5 and 3.1, respectively. Therefore, the presence of DMSO appeared to promote more compactness in the structures of the mutants compared to the effect of the mutations alone in water, especially with regard to M35A. Once transferred from DMSO into water, the wild-type, N27A, and M35A structures exhibited reductions in their average H-bond numbers of 2.0, 1.5, and 1.8, respectively, compared with those before simulation in DMSO.

### Systems Equilibration

One method to investigate the accuracy of MD simulation is the calculation of the autocorrelation function [39,40]. Therefore, the equilibrium behavior of the peptides was determined *via* the autocorrelation function of H-bonds

for conformations obtained by MD simulations for comparison and the quantities are shown in Fig. 7. The results show that the autocorrelation functions for all simulated peptides were fluctuating around 0, indicating that their overall structures were well-equilibrated.

### Compactness and Surface Properties

Protein structure compactness could be evaluated by calculating radius of gyration [41]. Figure 8 illustrates the gyration radii of the peptides during the simulations. In the initial water system, the gyration radii of all peptides revealed fluctuations around the same average value of  $0.65 \pm 0.11$  nm. The structural fluctuations were minimal for M35A from 100 to 160 ns, in which the largest cluster containing  $\beta$ -sheet structure was formed. In DMSO, the

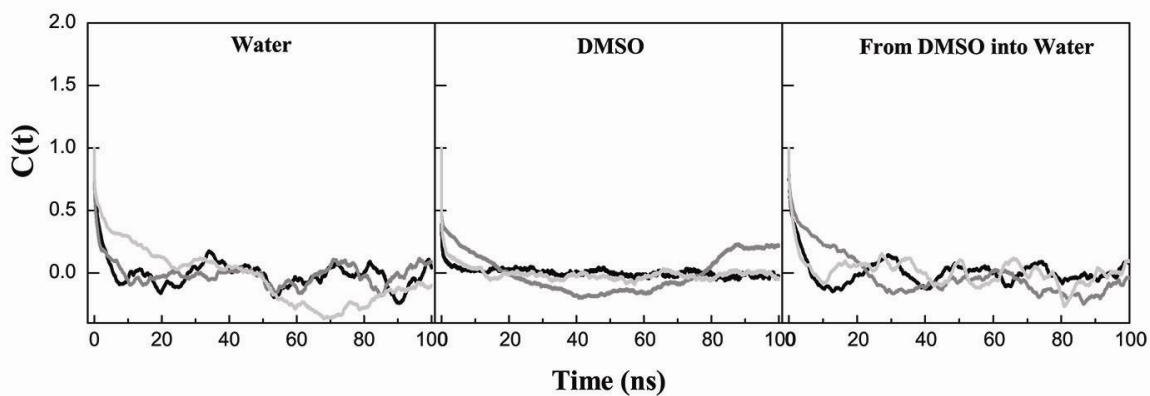


**Fig. 7.** Autocorrelation function of H-bonds. Autocorrelation function of H-bonds as a function of time ( $C(t)$ ) calculated for the simulations of the wild-type (black), N27A (gray), and M35A (light gray) structures of A $\beta$ (25-35) in pure water (left graph), pure DMSO (middle graph), and from pure DMSO into pure water (right graph).

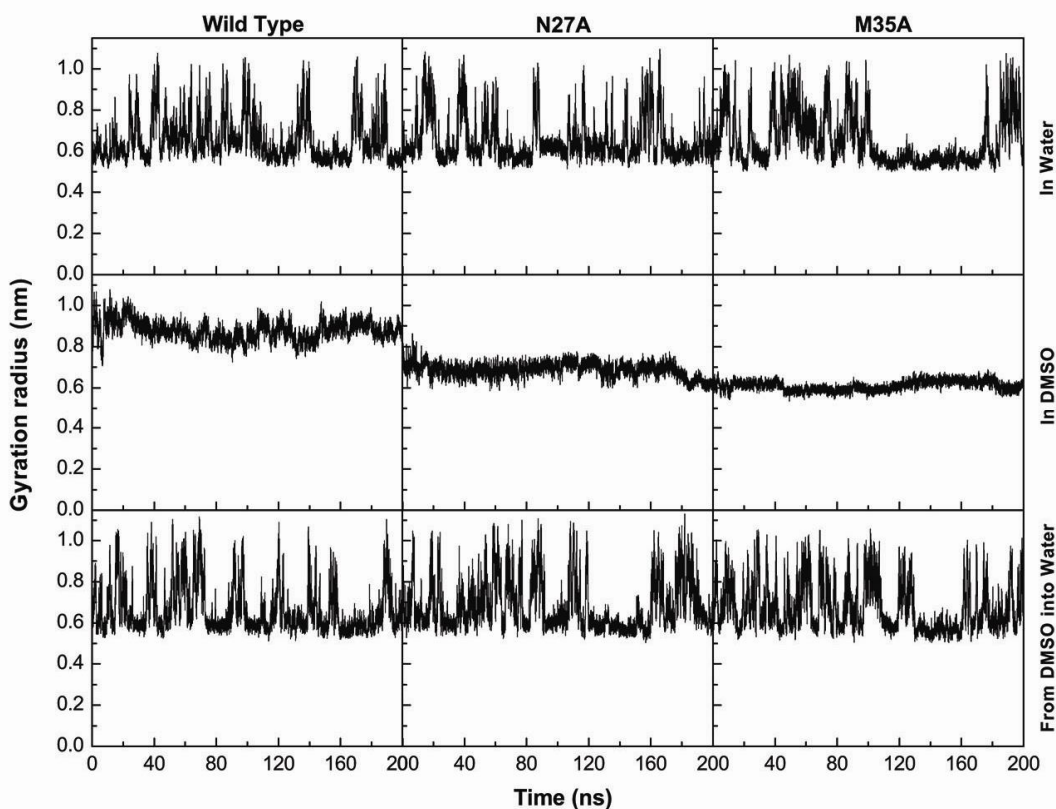


**Fig. 8.** Temporal changes of gyration radii of the wild-type (left column), N27A (middle column), and M35A (right column) peptides during the 200-ns MD simulations in pure water (top row), pure DMSO (middle row), and from pure DMSO into pure water (bottom row).

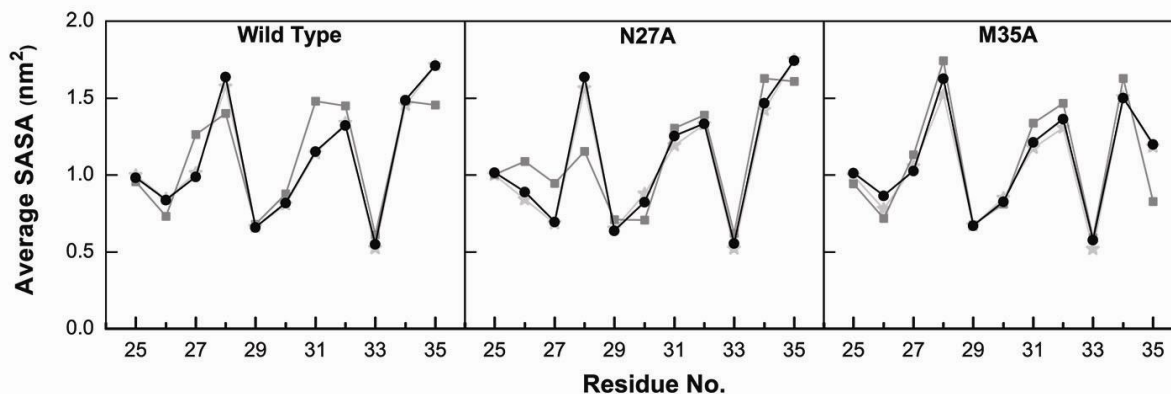


**Fig. 9.** Average values of Solvent Accessible Surface Area (SASA) calculated per residue of the wild-type and mutant structures of A $\beta$ (25-35) over the 200-ns simulation in pure water (light gray), pure DMSO (gray), and in pure water after being simulated in pure DMSO (black). The graphs of water systems, before and after treatment with DMSO, are mostly superimposed.

average gyration radius of the wild-type ( $0.88 \pm 0.05$  nm) and N27A ( $0.69 \pm 0.03$  nm) increased whereas these values decreased in M35A ( $0.61 \pm 0.02$  nm) as compared to initial water systems. When transferred from DMSO to water, the gyration radii of the wild-type, N27A, and M35A peptides demonstrated average values of  $0.67 \pm 0.11$ ,  $0.68 \pm 0.12$ ,  $0.67 \pm 0.11$  nm, respectively, which were slightly larger than those in initial water simulations. The combined effect of M35A mutation and DMSO appeared to result in the most compactness of this mutant whereas DMSO caused the least packing in the wild-type among all nine simulations.

In order to investigate further changes in peptide structure caused by DMSO, the average residual Solvent Accessible Surface Areas (SASAs) were calculated (Fig. 9). Higher SASA values imply greater exposure to the solvent. Interestingly, each peptide followed the same pattern of SASAs per residue in water systems, before and after exposure to DMSO. When N27A was compared to the wild-type peptide in all water systems, Ala27 demonstrated a notable decrease (from  $1.0$  nm<sup>2</sup> to  $0.69$  nm<sup>2</sup>) in its average SASA values and thus less exposure to water molecules. With respect to M35A, only average SASA of Ala35 decreased significantly compared to other peptides in all solvents indicating its high tendency to be buried. On the other hand, significant alterations in the average residual SASAs of the peptides were observed in DMSO. In the wild-type peptide, the average residual SASAs of Ser26,

Lys28, and Met35 decreased ( $0.1$ - $0.3$  nm<sup>2</sup>) in DMSO as compared to water systems, whereas these values increased for Asn27, Ile31, and Ile32 ( $0.1$ - $0.3$  nm<sup>2</sup>). With respect to N27A mutant, Ala27 and Lys28 demonstrated lower exposure to DMSO compared to other peptides in the same medium. In this case, N27A mutation made the adjacent residue (Lys28) become more buried compared to other peptides. Regarding M35A mutant in DMSO, the average SASA values of most residues followed the same pattern as the water simulations except for Ala35 which indicated a notable burial (a dramatic decrease in its SASA) as compared to other peptides. The fact that the wild-type peptide followed the same pattern of SASAs in all water systems, before and after exposure to DMSO, indicated that pre-simulation in DMSO had no significant effects on the average SASA values of the peptides in the final water simulations; the substitutions were the only factors to induce changes in the average SASAs of the mutated residues. In the final water simulations, the substitutions in the mutants were the most buried residues with their average SASAs being notably reduced compared to the wild-type peptide. Overall, the more hydrophobic characteristics applied to the peptide, by introducing N27A mutation, was furthermore confirmed by observing lower exposure of Ala27 to either media (lower average SASA value of Ala27) as compared to other peptides in all simulation systems. In the less hydrophobic M35A mutant,

Ala35 was also buried from the solvent exposure with a considerable decrease in its average SASA value compared to the other two peptides.

## DISCUSSIONS

The purpose of this investigation was to determine the initial structural effects of two factors on A $\beta$ (25-35) monomer at atomic scale: DMSO as solvent, and two N27A and M35A mutations with different degrees of hydrophobicity. Even though full length A $\beta$  is considered as the principal peptide in the brain tissues of affected patients, A $\beta$ (25-35) is regarded as its neurotoxic core while being even more toxic than the parent peptide [42]. A $\beta$ (25-35) has received particular interest by showing the ability to form consistent  $\beta$ -sheet aggregates and retain similar toxicity of the full-length peptide [11,14,43]. Meanwhile, Gruden *et. al* proved the presence of A $\beta$ (25-35) aggregates in patients with progressive AD [13], suggesting that A $\beta$ (25-35) may be related to Alzheimer's disease pathogenicity [10,14]. Various studies have also demonstrated that the aggregation state of A $\beta$ (25-35) is crucial for its ability to induce toxicity [9], such as membrane perturbation [8] and mitochondria loss and malfunction [8,44,45]. Therefore, A $\beta$ (25-35) could be a reliable representative of full-length A $\beta$  in structural and functional studies by retaining both the physical and biological properties of intact A $\beta$ .

In simulating wild-type A $\beta$ (25-35) and its two mutants in pure water, pure DMSO, and from pure DMSO into pure water, some notable results were obtained. The accuracy of MD simulations and the equilibrium behavior of the peptides were initially determined *via* the autocorrelation function of H-bonds (Fig. 7). Based on DSSP data, wild-type A $\beta$ (25-35) showed unordered structure when first dissolved in pure water which was previously observed in our experimental study [8]. At the temperature of 310 K, the wild-type peptide adopted two antiparallel  $\beta$ -strands along with coil and turn structures in pure water which was in accordance with the study of Wei and Shea when they simulated A $\beta$ (25-35) sequence in water at 300 K [18]. This indicated that the difference of 10 K in the simulation temperature performed in our case compared to Wei's study did not affect the dominant conformations of A $\beta$ (25-35) sequence in pure water. In addition, Particle Mesh Ewald

(PME) method [36] was employed in this study to calculate the electrostatic interactions. A neutral system is required for use of the PME method, therefore suitable counter ions were added to neutralize the charge of the protein in the system [46-48]. Ibragimova and Wade have demonstrated that the usual procedure of only placing a few charge-balancing counter ions near charged groups on the protein surface did not disturb the stability of the protein, but full ionic strength (at 0.2 M) was necessary in order to affect the protein stability [46].

In the first set of simulations of the mutant peptides performed in pure water, the less hydrophobic M35A seemed to be more compact in structure than N27A, confirmed by showing a higher average H-bond number and DSSP results. Even though N27A mutant is more hydrophobic in nature than M35A, the formation of  $\beta$  structures was significantly increased in the M35A mutant in pure water. The presence of high  $\beta$ -sheet content is a proved characteristic of aggregates [1,3]. The  $\beta$ -sheet-rich structure of M35A, compared to N27A, could make this mutant more aggregation-prone. This phenomenon was proved in another study indicating that N27A did not readily aggregate whereas M35A showed significant aggregation [49]. Introducing hydrophobic mutation at the peptide terminal, compared to internal mutation, seemed to make it more feasible for the peptide to fold back into  $\beta$  secondary structure and maintain the folded structure for a longer time. The conformation of A $\beta$ (25-35) generated through MD simulations seemed to be highly dependent on DMSO. Amyloid peptides have been experimentally proved to be less prone to form aggregates in DMSO stock solution, even after further dilution in aqueous media [22,50,51]. At high concentrations of DMSO, A $\beta$ 40 and A $\beta$ 42 peptides have shown to be predominantly monomers or oligomers, whereas decreasing DMSO concentration has proved to increase the fibrillar form [52]. Therefore, published methods suggest preparation of stock solutions of A $\beta$  peptide in DMSO, before dilution into an aqueous buffer medium, to induce proper folding [21]. In the present study, solvating the wild-type A $\beta$ (25-35) in 100% DMSO caused drastic reduction in the number of hydrogen bonds and unfolding in the peptide, as confirmed by DSSP analysis and the increase observed in values of average gyration radius. In general, pure DMSO unfolded the structures of all

three simulated peptides to mainly bend and coil structures. It is shown that at higher DMSO concentrations (above 75%), intramolecular C=O...H<sub>2</sub>-N hydrogen bonds of proteins break due to the formation of DMS=O...H<sub>2</sub>-N-protein hydrogen bonds, inducing unfolding of the protein chain. In this case, fibrillar structures dissociate by further disruption of the intermolecular hydrogen bonds [23]. In our study, the starting structures of the wild-type and M35A peptides were helices in 100% DMSO; however, pure DMSO caused unfolding of their secondary structures. It has been demonstrated that 100% DMSO solutions destabilize  $\alpha$ -helices completely [24] presumably by competing with the carboxyl groups of the peptides to make hydrogen bonds with the peptides amine groups [23]. Moreover, the small relative dielectric constant ( $\epsilon = 46.8$ ) of DMSO has enabled it to solubilize hydrophobic helical peptides [23]. Therefore, pure DMSO can lead to unfolding [23,50] and loss of secondary structure in proteins [23] which was also observed in our study. In addition, the hydrophobic methyl groups of DMSO have shown the ability of interacting with hydrophobic side chains of the A $\beta$  peptide and to completely dissociate amyloid fibrils by destructing the hydrogen bond network [22]. This explains the significant decrease in the average H-bond number in the wild-type peptide once simulated in pure DMSO in this study.

Interestingly, with regard to both mutants, the number of hydrogen bonds significantly increased and their structures became more compact than the wild-type peptide in pure DMSO, as confirmed by both their lower average gyration radii and DSSP analyses. In this case, the hydrophobic characteristics of the mutants seemed to overcome the ability of DMSO to solubilize them. Therefore, higher numbers of hydrogen bonds have formed within the mutants in order to bury the hydrophobic residues, which is in accordance with the decrease in the solvent accessible surface areas of the mutated residues. The presence of both DMSO and M35A mutation also seemed to cause more compactness relative to N27A mutation, while the effect of DMSO on the wild-type peptide was the opposite.

Based on the results obtained from RMSD and RMSF analyses, dynamics of all peptides' backbones, regardless of the applied mutations, were considerably decreased in pure DMSO possibly due to the small dielectric constant of DMSO [62]. Early MD simulations have also shown that a

protein rate of motion is dependent on the dielectric constant of the solvent, and protein motion is slower in hydrophobic (lower dielectric constant) solvents [53].

Interestingly, pure DMSO in combination with M35A mutation conferred a more pronounced enhancement on the stability of this mutant, compared to N27A, by demonstrating the lowest values of average backbone motion and lower number of formed clusters. The mechanism of the effects of DMSO on protein conformational stability is not well-understood [54]. However, significant flexibility reduction (reduction in RMSF values) of four amino acids of M35A in pure DMSO could be responsible for conferring such stability: K28, G29, A30, and G33. Some studies have shown that the interactions of glycine and polar amino acids with DMSO are highly unfavorable and this unfavorable interaction increases sharply at higher DMSO concentrations [54]. There are two glycine and one polar lysine residues among the four mentioned amino acids with reduced flexibility. It seems that at 100% DMSO, the majority of these four amino acids (3 out of 4) in the central segment of M35A did not establish favorable binding with DMSO which induced lowered fluctuations and consequently increased stability. It should be noted that in M35A, there was polar Asn27 placed before polar Lys28 which conferred more to unfavorable interaction with pure DMSO; however, in N27A, there was hydrophobic Ala27 placed before the middle segment which could establish favorable interaction with hydrophobic DMSO solvent [54].

In A $\beta$ (25-35) sequence, Asn27 and particularly Met35 residues have played crucial roles in the peptide structure [25,49]. In the present study, application of N27A and M35A mutations increased hydrophobicity in the wild-type peptide and consequently increased the tendency of the structure to be more buried away from water. This observation was further confirmed by previous simulation studies demonstrating that the more hydrophobic N27A peptide favored the low-dielectric membrane environment whereas the less hydrophobic M35A peptide preferred the high-dielectric aqueous phase [25]. Regarding toxicity-hydrophobicity relationship, Sato *et al.* demonstrated that mutation of Asn27 residue in A $\beta$ (25-35) peptide to alanine produced an increased hydrophobic analog with a much weaker toxicity than that of A $\beta$ (25-35). On the other hand, a

replacement of Met35 residue in A $\beta$ (25-35) peptide with alanine yielded a less hydrophobic, but more toxic analog [49]. It was also indicated that less toxic N27A did not readily aggregate whereas toxic M35A showed significant aggregation, which was in accordance with the higher  $\beta$ -sheet contents obtained for M35A compared to N27A in our initial water simulations (Fig. 5). More specifically, the 33-35 region of A $\beta$ (1-42) has been shown to be critical for the aggregation and neurotoxic properties of this peptide [55]. It was therefore declared that it was not the peptide hydrophobicity but the degree of peptide aggregation via intermolecular  $\beta$ -sheet formation that made A $\beta$ (25-35) analogs toxic [49].

## CONCLUSIONS

In the present work, early stages of A $\beta$ (25-35) folding were investigated in the presence of two mutations (N27A and M35A) in pure water, before and after exposure to pure DMSO, by applying molecular dynamics simulations. The results revealed that hydrophobic N27A and M35A mutations applied to wild-type A $\beta$ (25-35) reduced the flexibility of the peptides. When the mutation was applied at the peptide terminal, rather than internally, the less hydrophobic M35A mutant seemed to get more compact in structure with a greater tendency to form more  $\beta$  secondary structure and maintain the folded structure for a longer time throughout the simulation courses. Meanwhile, pure DMSO reduced the peptides' dynamics dramatically. Although pure DMSO is expected to cause loss of secondary structure in proteins and consequently a decrease in their compactness, the hydrophobic characteristics of mutations seemed to overcome the solvent effect noticeably by showing less exposure to DMSO while making more hydrogen bonds within mutants' structures. Moreover, pre-treatment with DMSO caused a general delay and notable reduction in  $\beta$ -structure formation in all three peptides. This study helps to unmask and prevent experimental artifacts by demonstrating how pretreatment in DMSO would limit beta-structure formation in experiments.

## ACKNOWLEDGMENTS

This study was supported by the Research Council of

the University of Tehran with the grant No. 6401007-6-18. The authors declare to have no conflict of interest and would like to thank Ms. Mahshid Shafizadeh at Institute of Biochemistry and Biophysics, University of Tehran, for her technical support.

## REFERENCES

- [1] F. Chiti, C.M. Dobson, *Annu. Rev. Biochem.* 75 (2006) 333.
- [2] C.M. Dobson, *Nat. Rev. Drug Discov.* 2 (2003) 154.
- [3] M. Stefani, C.M. Dobson, *J. Mol. Med.* 81 (2003) 678.
- [4] V. Cavallucci, M. D'Amelio, F. Cecconi, *Mol. Neurobiol.* 45 (2012) 366.
- [5] R.J. O'Brien, P.C. Wong, *Annu. Rev. Neurosci.* 34 (2011) 185.
- [6] C. Hilbich, B. Kisters-Woike, J. Reed, C.L. Masters, K. Beyreuther, *J. Mol. Biol.* 218 (1991) 149.
- [7] C.J. Pike, A.J. Walencewicz-Wasserman, J. Kosmoski, D.H. Cribbs, C.G. Glabe, C.W. Cotman, *J. Neurochem.* 64 (1995) 253.
- [8] M. Ghobeh, S. Ahmadian, A.A. Meratan, A. Ebrahim-Habibi, A. Ghasemi, M. Shafizadeh, M. Nemat-Gorgani, *Peptide Sci.* 102 (2014) 473.
- [9] M. Hashimoto, M. Katakura, S. Hossain, A. Rahman, T. Shimada, O. Shido, *J. Nutr. Biochem.* 22 (2011) 22.
- [10] T. Kubo, S. Nishimura, Y. Kumagae, I. Kaneko, *J. Neurosci. Res.* 70 (2002) 474.
- [11] J. Xu, S. Chen, S.H. Ahmed, H. Chen, G. Ku, M.P. Goldberg, C.Y. Hsu, *J. Neurosci.* 21 (2001) RC118.
- [12] M.E. Clementi, S. Marini, M. Coletta, F. Orsini, B. Giardina, F. Misi, *FEBS Lett.* 579 (2005) 2913.
- [13] M.A. Gruden, T.B. Davudova, M. Mališauskas, V.V. Zamotin, R.D.E. Sewell, N.I. Voskresenskaya, I.A. Kostanyan, V.V. Sherstnev, L.A. Morozova-Roche, *Dement. Geriatr. Cogn. Disord.* 18 (2004) 165.
- [14] Y.G. Kaminsky, M.W. Marlatt, M.A. Smith, E.A. Kosenko, *Exp. Neurol.* 221 (2010) 26.
- [15] K.F. DuBay, A.P. Pawar, F. Chiti, J. Zurdo, C.M. Dobson, M., Vendruscolo, *J. Mol. Biol.* 341 (2004) 1317.

- [16] A.M. Fernandez-Escamilla, F. Rousseau, J. Schymkowitz, L. Serrano, *Nat. Biotechnol.* 22 (2004) 1302.
- [17] R. Linding, J. Schymkowitz, F. Rousseau, F. Diella, L. Serrano, *J. Mol. Biol.* 342 (2004) 345.
- [18] G. Wei, J.E. Shea, *Biophys. J.* 91 (2006) 1638.
- [19] H. LeVine, *Anal. Biochem.* 335 (2004) 81.
- [20] L. Millucci, R. Raggiaschi, D. Franceschini, G. Terstappen, A. Santucci, *J. Biosci.* 34 (2009) 293.
- [21] G. Bitan, D.B. Teplow, *Methods Mol. Biol.* 299 (2005) 3.
- [22] K. Broersen, W. Jonckheere, J. Rozenski, A. Vandersteen, K. Pauwels, A. Pastore, F. Rousseau, J. Schymkowitz, *Protein Eng. Des. Sel.* 24 (2011) 743.
- [23] M. Jackson, H.H. Mantsch, *Biochim. Biophys. Acta* 1078 (1991) 231.
- [24] A.N.L. Batista, J.M. Batista, V.S. Bolzani, M. Furlan, E.W. Blanch, *Phys. Chem. Chem. Phys.* 15 (2013) 20147.
- [25] H.H. Tsai, J.B. Lee, S.S. Tseng, X.A. Pan, Y.C. Shih, *Proteins* 78 (2010) 1909.
- [26] G. Wei, A.I. Jewett, J.E. Shea, *Phys. Chem. Phys.* 12 (2010) 3622.
- [27] C. Wurth, N.K. Guimard, M.H. Hecht, *J. Mol. Biol.* 319 (2002) 1279.
- [28] A.M. D'Ursi, M.R. Armenante, R. Guerrini, S. Salvadori, G. Sorrentino, D. Picone, *J. Med. Chem.* 47 (2004) 4231.
- [29] H.J.C. Berendsen, J.R. Grigera, T.P. Straatsma, *J. Phys. Chem.* 91 (1987) 6269.
- [30] D.P. Geerke, C. Oostenbrink, N.F. van der Vegt, W.F. van Gunsteren, *J. Phys. Chem. B* 108 (2004) 1436.
- [31] E. Apol, R. Apostolov, H.J.C. Berendsen, A. Van Buuren, P. Bjelkmar, R. Van Drunen, A. Feenstra, e.a., *GROMACS user manual version 4.5.4.* 2010.
- [32] C. Oostenbrink, A. Villa, A.E. Mark, W.F. van Gunsteren, *J. Comput. Chem.* 25 (2004) 1656.
- [33] G. Bussi, D. Donadio, M. Parrinello, *J. Chem. Phys.* 126 (2007) 014101.
- [34] M. Parrinello, A. Rahman, *J. Appl. Phys.* 52 (1981) 7182.
- [35] B. Hess, H. Bekker, H.J. Berendsen, J.G. Fraaije, *J. Comput. Chem.* 18 (1997) 1463.
- [36] T. Darden, D. York, L. Pedersen, *J. Chem. Phys.* 98 (1993) 10089.
- [37] W. Kabsch, C. Sander, *Biopolymers* 22 (1983) 2577.
- [38] W. Humphrey, A. Dalke, K. Schulten, *Molec. Graphics* 14 (1996) 33.
- [39] W. Zhang, C. Wu, Y. Duan, *J. Chem. Phys.* 123 (2005) 154105.
- [40] J.D. Chodera, W.C. Swope, J.W. Pitera, C. Seok, K.A. Dill, *J. Chem. Theory Comput.* 3 (2007) 26.
- [41] M.Y. Lobanov, N.S. Bogatyreva, O.V. Galzitskaya, *Mol. Biology* 42 (2008) 623.
- [42] S. Varadarajan, J. Kanski, M. Aksenova, C. Lauderback, D.A. Butterfield, *J. Am. Chem. Soc.* 123 (2001) 5625.
- [43] C.S. Casley, J.M. Land, M.A. Sharpe, J.B. Clark, M.R. Duchon, L. Canevari, *Neurobiol. Dis.* 10 (2002) 258.
- [44] J.X. Chen, S.S. Yan, *J. Alzheimers Dis.* 20 (2010) 569.
- [45] L. Tillement, L. Lecanu, V. Papadopoulos, *Neurodegener. Dis.* 8 (2011) 331.
- [46] G.T. Ibragimova, R.C. Wade, *Biophys. J.* 74 (1998) 2906.
- [47] P. Drabik, A. Liwo, C. Czaplewski, J. Ciarkowski, *Protein Eng. Des. Sel.* 14 (2001) 747.
- [48] Y. Yu, J. Wang, Q. Shao, J. Shi, W. Zhu, *Scientific Reports* 1 (2016) 6.
- [49] K. Sato, A. Wakamiya, T. Maeda, K. Noguchi, A. Takashima, K. Imahori, *J. Biochem.* 118 (1995) 1108.
- [50] T. Arakawa, Y. Kita, S.N. Timasheff, *Biophys. Chem.* 131 (2007) 62.
- [51] W.B. Stine, K.N. Dahlgren, G.A. Krafft, M.J. LaDu, *J. Biol. Chem.* 278 (2003) 11612.
- [52] A. Jan, D.M. Hartley, H.A. Lashuel, *Nat. Protoc.* 5 (2010) 1186.
- [53] R. Affleck, C.A. Haynes, D.S. Clark, *Proc. Natl. Acad. Sci. USA* 89 (1992) 5167.
- [54] T. Arakawa, Y. Kita, S.N. Timasheff, *Biophys. Chem.* 131 (2007) 62.
- [55] D.A. Butterfield, R. Sultana, *J. Amino Acids* (2011) ID 198430.